Twelfth Australasian Fluid Mechanics Conference
The University of Sydney, Australia 1995

MODELLING 3D TURBULENT FLOW IN A CONTINUOUS CASTING TUNDISH USING FASTFLO

Xiao-Lin LUO
CSIRO Division of Mathematics and Statistics
Sydney, New South Wales
AUSTRALIA

ABSTRACT

Fastflo was used to simulate the 3D turbulent flow in a continuous casting tundish, and subsequently the transient transportation of the dye injected into the steady flow field. The predicted minimum residence time of dye injection agrees well with the water model experiments conducted by BHP Research. Animation of the isosurfaces of the dye concentration computed from the transient simulation reveals flow details having strong resemblance to the observed features in the dye injection experiments, notably the stalling and floor 'short-circuiting' of the dye concentration front.

1. INTRODUCTION

A continuous casting tundish is a final vessel in the steelmaking process where adjustments can be made to steel chemistry, temperature and cleanliness. Increasingly, the tundish is no longer seen as just a liquid steel distributor but as a full treatment vessel in the making of cleaner steels (Heaslip et al., 1990). A better understanding of the liquid steel flow within the tundish is of great importance for quality and productivity improvements of steelmaking. Mathematical modelling has served as a research tool integrated with water modelling studies aimed at improving tundish design and operations (Salvati et al., 1991, Lewis, 1993).

Fastflo is a finite element based pde solver for CFD, developed at the Division of Mathematics and Statistics, CSIRO, and it supports a high level control language called *Fasttalk*. The present work applies *Fastflo*'s turbulence module to solve the tundish flow problem, and compares numerical results with data and observations from the water modeling experiments of BHP Research.

2. GOVERNING EQUATIONS

The turbulent flow of an incompressible viscous fluid is modelled by the Reynolds-averaged Navier-Stokes equation and the continuity equation

$$\frac{\partial \mathrm{u}}{\partial t} + (\mathrm{u}\cdot\nabla)\mathrm{u} + \frac{\nabla p}{\rho} - \nabla\cdot[\nu(\nabla\mathrm{u} + \nabla^T\mathrm{u})] = 0 \quad (1)$$

$$\nabla\cdot\mathrm{u} = 0 \quad (2)$$

where ρ is the fluid density, u is the mean velocity, p is the mean pressure, and $\nu = \nu_0 + \nu_t$ is the sum of the laminar and turbulent viscosities. The turbulent viscosity is given by

$$\nu_t = C_\mu \frac{k^2}{\epsilon} \quad (3)$$

where k and ϵ are the turbulent kinetic energy and dissipation rate respectively. The standard k-ϵ model (Launder and Spalding, 1974) gives

$$\frac{\partial k}{\partial t} + (\mathrm{u}.\nabla)k - \nabla.(\nu_k\nabla k) + \epsilon = G \quad (4)$$

$$\frac{\partial \epsilon}{\partial t} + (\mathrm{u}.\nabla)\epsilon - \nabla.(\nu_\epsilon\nabla\epsilon) + C_2\frac{\epsilon^2}{k} = C_1\frac{\epsilon}{k}G \quad (5)$$

where $\nu_k = \nu_0 + \frac{\nu_t}{\sigma_k}$, $\nu_\epsilon = \nu_0 + \frac{\nu_t}{\sigma_\epsilon}$ and G is the turbulent generation term. The constants in equations (3–5) take the standard values.

For turbulent viscosity near a wall, the van Driest (1956) mixing length approach is adopted here:

$$\nu_t = l_m^2[(\frac{\partial u_i}{\partial x_j} + \frac{\partial u_j}{\partial x_i})\frac{\partial u_i}{\partial x_j}]^{1/2} \qquad (6)$$

where l_m is the mixing length obtained from van Driest's equation.

For species concentration, the turbulent diffusion process is modelled as

$$\frac{\partial C}{\partial t} + (\mathrm{u}.\nabla)C - \nabla.[(\frac{\nu_t}{\sigma_t})\nabla C] = 0 \qquad (7)$$

where σ_t is the flow dependent turbulent Prandtl number in the order of unity.

3. OPERATOR SPLITTING ALGORITHM

The following segregated time stepping scheme is used to solve the coupled nonlinear system of the k-ϵ turbulence model:

1) Solve for $\{\mathrm{u}^{n+1}, p^{n+1}\}$ the Reynolds avereaged momentum equations by operator splitting in three fractional steps.

First fractional step:

$$\begin{array}{c} \frac{\mathrm{u}^{n+\theta}-\mathrm{u}^n}{\theta\Delta t} - \alpha\nabla\cdot(\nu^n\nabla\mathrm{u}^{n+\theta}) \\ +\nabla p^{n+\theta} = \beta\nabla\cdot(\nu^n\nabla\mathrm{u}^n) \\ -(\mathrm{u}^n\cdot\nabla)\mathrm{u}^n + \nabla\cdot(\nu^n(\nabla\mathrm{u}^n)^T) \end{array} \qquad (8)$$

$$\nabla\cdot\mathrm{u}^{n+\theta} = 0 \qquad (9)$$

where α, β and θ are the operator splitting parameters satisfying $\alpha+\beta=1$ and $0<\theta<1$.

Second fractional step:

$$\begin{array}{c} \frac{\mathrm{u}^{n+1-\theta}-\mathrm{u}^{n+\theta}}{(1-2\theta)\Delta t} - \beta\nabla\cdot(\nu^n\nabla\mathrm{u}^{n+1-\theta}) + \\ (\mathrm{u}^{n+\theta}\cdot\nabla)\mathrm{u}^{n+1-\theta} + \nabla\cdot(\nu^n(\nabla\mathrm{u}^{n+1-\theta})^T) \\ = \alpha\nabla\cdot(\nu^n\nabla\mathrm{u}^{n+\theta}) - \nabla p^{n+\theta} \end{array} \qquad (10)$$

Third fractional step: *equivalent to the first*

2) Solve for k-ϵ by a semi-implicit or fully implicit method.

The sub-problems at first and third fractional steps are a type of steady Stokes problem, which can be solved by a preconditioned conjugate gradient method (Glowinski et al., 1988, 1991). The sub-problem at the second fractional step is linearized and can be solved directly. After obtaining the steady state solutions for k, ϵ, u and p, the transient dye injection problem is solved by a Crank-Nicolson scheme. Iterative solvers have been used for all the resulting linear systems, with conjugate gradient (CG) method for symmetric systems and generalized minimal residual (GMRES) method for asymmetric systems. An ILU precondition was used for both cases.

4. NUMERICAL RESULTS

The finite element mesh for the tundish geometry is shown in Fig. 1. Only half of the tundish is concerned in the computation since a symmetry plane exists on its longitudinal axis. The longitudinal length is about 4.5 meters. This mesh contains 7210 bricks with a total of 33389 nodes.

The top horizontal plane is a fixed surface in which fluid can move freely. The inlet delivery nozzle, near the top right corner in the symmetry (front) plane, is submerged in the liquid and the flow coming from the nozzle is fully turbulent. Plug flow was assumed at the inlet, and zero normal stress gradient at the outlet, which is located near the bottom left corner in the symmetry plane. The Reynolds number based on nozzle diameter and inlet velocity is 170,000. On solid walls, a no-slip BC was imposed for velocity, and the van Driest wall function was used for the turbulent viscosity in the viscous sub-layer. Boundary conditions for $k-\epsilon$ on top of wall elements were:

$$\frac{\partial k}{\partial n} = 0, \quad \epsilon = \frac{C_\mu^{0.75}k^{1.5}}{\kappa\delta} \qquad (11)$$

On outlet and symmetry planes we had

$$\frac{\partial k}{\partial n} = 0, \quad \frac{\partial \epsilon}{\partial n} = 0 \qquad (12)$$

and at inlet,

$$k_{in} = C_{p1}u_{in}^2\ ; \quad \epsilon_{in} = \frac{k_{in}^{1.5}}{C_{p2}D} \qquad (13)$$

where u_{in} is the mean inlet velocity, D is the hydraulic diameter and C_{p1} and C_{p2} are empirical constants with values 0.005 and 0.3 respectively.

Fig. 2 shows velocity field in the free surface and in the symmetry plane at a flowrate $Q = 523(l/min)$. The flow is characterised by a strong impinging jet and recirculation near the inlet.

In the experiment the dye injection lasted 8 seconds, which dictated a step function of time as the boundary condition at inlet for the dye concentration. The primary interest here is to determine the minimum residence time (MRT) of the dye, which is defined as the time it takes to reach 5% of the peak concentration at the outlet. More than one thousand time steps were required

to predict MRT, since not only the peak value of concentration at outlet typically took several hundred seconds to reach, but also a small time step was required for time accuracy (in the order of 0.1 sec.), at least for the first 30 seconds or so, in order to capture the initial impinging of the dye injection. However, the computing expense was greatly reduced by saving and reusing the incomplete preconditioning factors for all time steps with fixed dt, taking advantage of the unchanged LHS matrix due to the flow being steady and making use of *Fastflo*'s matrix storage/recovery commands.

Table 1 compares the predicted residence time ($T_{num.}$) with the water model experiment data ($T_{exp.}$) at two flowrates (Q). While the agreement is good, the calculations predicted slightly longer residence time. Also shown in the table are the predicted values of peak concentration at outlet (C_{max}) and the time it took to reach the peak value (T_{max}).

Fig. 3 plots the iso-surface of 2% dye concentration after 30 seconds (full geometry view). The figure clearly shows a tendency for the dye front to bend upstream towards the inlet at the tundish floor and near the symmetry plane, forming a 'short circuiting'. Further more, animation of the time dependent solution up to the first 60 seconds shows the dye front actually stalled, barely moving after the first 20 seconds or so. These features have strong resemblance to experimental observations.

CONCLUSIONS

Full numerical simulation of three dimensional turbulent flow in the continuous casting tundish has been performed using *Fastflo*. Good convergence to a steady state solution has been obtained efficiently by applying the operator splitting algorithm. Transient simulation of the dye injection has revealed greater insight into characteristics of the turbulent flow field and the associated turbulent diffusion process.

To improve the transient dye injection modelling, a more refined turbulent diffusion model, which takes into consideration the different turbulent scales within and outside the impinging jet, is essential. Lagrangian stochastic models for particle motion in turbulent flow (Batchelor 1953, Thomson 1990, Borgas and Sawford 1994) may provide a better but more computing intensive alternative.

Table 1: DYE INJECTION MINIMUM RESIDENCE TIMES.

Q(l/min.)	$T_{exp.}$	$T_{num.}$	C_{max}	T_{max}
654	47 Sec.	51 Sec.	0.0122	368 Sec.
523	56 Sec.	59 Sec.	0.00929	454 Sec.

ACKNOWLEDGMENTS

This work is part of the *Fastflo* project carried out in CSIRO Division of Mathematics and Statistics, supported by the Australian Government, BHP and Compumod. The author wishes to thank Dr. John Truelove of BHP Research for providing experimental data and helpful discussions.

REFERENCES

Batchelor, G.K. *Proc. Camb. Phil. Soc.* 48, 345–362, 1952.

Borgas M.S. and Sawford B.L., *J. Fluid Mech. Vol.* 279, pp. 69–99, 1994.

Dean, E. Glowinski, R. Li, C.H. *Mathematics Applied to Science*, ed. Goldstein, J. Rosecrans, S. & Sod, G. 1988.

Glowinski, R. *Finite element methods for the Numerical Simulation of Incompressible Viscous Flow.* In Lectures in Applied Maths, Vol **28**, 1991.

Heaslip, L. J. et al., *48th Elec. Furnace Conf. Proc.*, New Orleans, Louisiana, USA, 113–117, 1990.

Launder BE and Spalding DB, Computer Methods in Applied Mechanics and Engineering 3 269–289, 1974.

Lewis A., BHP Technical Report, 1993.

Salvati F. et al., *1st Euro. Conf. Cont. Casting,* **2**, Florence, Italy, 23–25 Sept. 1991.

Thomson, D.J. *J. Fluid Mech. Vol.* 210, 113–153, 1990.

van Driest, E.R. *Journal of the Aeronautical Sciences,* Vol. 23, 1007–1011, 1956.

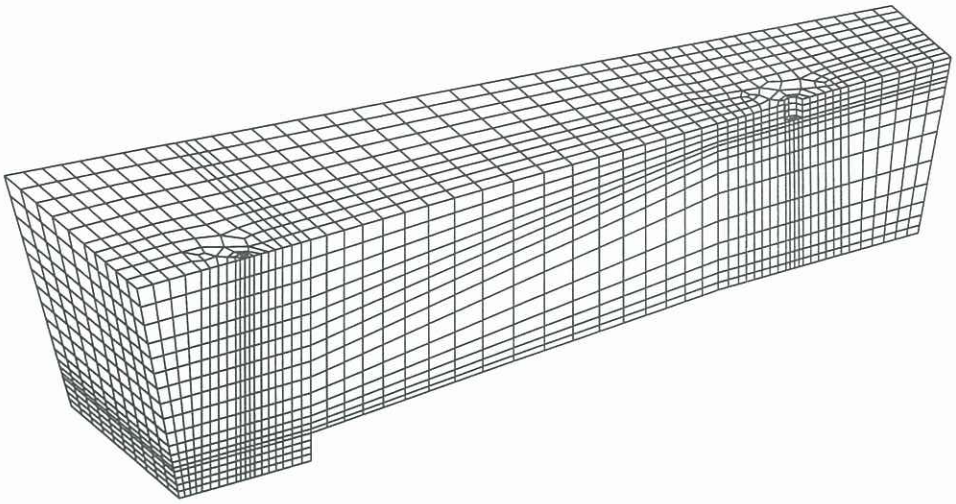

Fig. 1 TUNDISH GEOMETRY AND FINITE ELEMENT MESH.

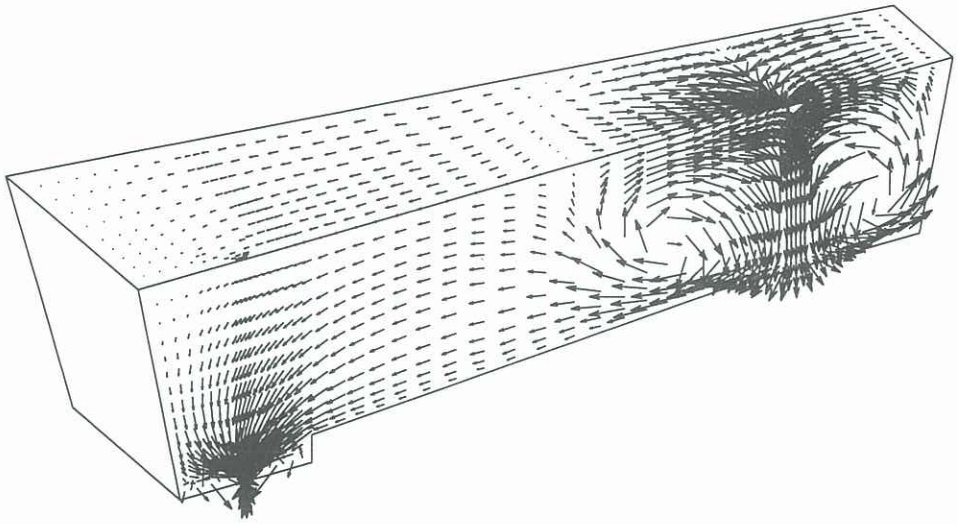

Fig.2 VELOCITY ON THE TOP FREE SURFACE AND ON THE SYMMETRY PLANE.

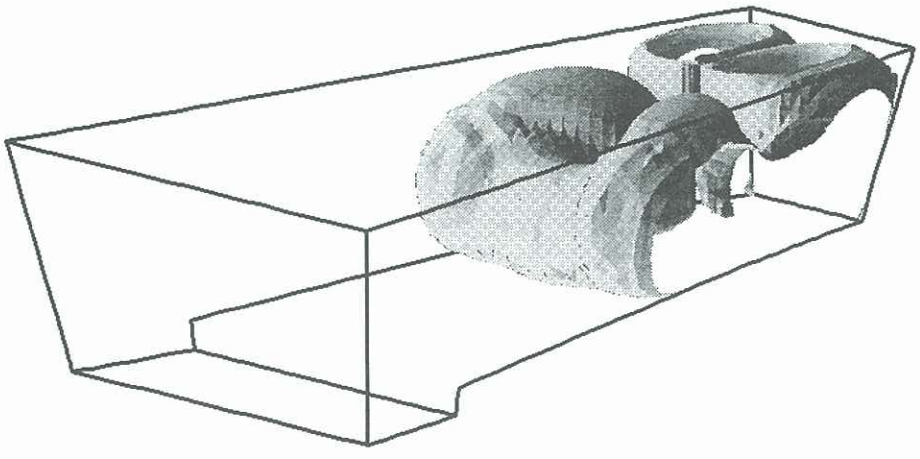

Fig.3 ISO-SURFACE OF 2% DYE CONCENTRATION AFTER 30 SECONDS.